



## CARBON PARTITIONING AND MECHANISM OF BAINITE REACTION IN EXPERIMENTAL Fe-Cr-Mo-C STEEL

Zdzisław Ławrynowicz

*University of Technology and Life Sciences, Mechanical Engineering Faculty  
Department of Materials Science and Engineering  
av. Kaliskiego 7, 85-789 Bydgoszcz, Poland  
E-mail: lawry@utp.edu.pl*

### **Abstract**

*Carbon partitioning and mechanism of bainite transformation have been studied in Fe-Cr-Mo-C steel using high speed dilatometry backed by thermodynamic analysis. Obtained results confirm the incomplete reaction phenomenon with the cessation of the bainite transformation well before paraequilibrium is achieved. These experimental data indicate that bainitic ferrite forms by a displacive transformation mechanism, but soon afterwards, excess of carbon is partitioned into the residual austenite. The results are discussed in terms of the mechanism of bainite transformation.*

**Keywords:** carbon partitioning, mechanism of bainite transformation

### **1. Introduction**

Carbon concentration in the residual austenite at the termination of the bainitic reaction and the mechanism of bainite transformation in steels remain still controversial and involves two general concepts, that bainitic reaction occurs via a diffusional mechanism [1], and that bainitic reaction occurs in a displacive mechanism as far as the substitutional elements are concerned [4]. Aaronson and co-workers introduced hypothesis that occurrence of bainitic "bay" on *TTT* diagrams many commercial steels and incomplete reaction phenomenon (transformation stasis) are attributed to a special effect of alloying elements on the growth kinetics, which was termed as a solute drag-like effect (SDLE) [3,6,9,17]. However, atom probe experiments reveal the absence of any substitutional alloying element partitioning at the bainitic ferrite/austenite interface during bainitic transformation. It is usually assumed that the point where dimensions cease to change represents full transformation. But in case of bainitic transformation, reaction ceases before the parent phase has completely transformed what is known as an incomplete reaction phenomenon. It means that at any temperature below  $B_S$  and in the absence of any interfering secondary reactions only a limited quantity of bainitic ferrite forms before the reaction terminates. The role of carbon in the growth of bainite, is difficult to resolve directly, because even if the ferrite is supersaturated during growth, the relatively high transformation

temperatures provide an opportunity for the excess of carbon to diffuse rapidly into residual austenite before any experimental measurements can be made [2]. There are indirect methods of determining the carbon concentration of bainitic ferrite during growth, e.g. dilatometry method. This paper attempts to investigate the mechanism of the bainite transformation in 15HM2 steel and to clarify the bainitic ferrite formation mechanism from the thermodynamic point of view.

## 2. Experimental procedures

A high-speed Adamel Lhomargy LK-02 dilatometer was used to establish change of length ( $\Delta L/L$ ) during isothermal bainitic transformation. In order to ensure rapid cooling ( $\sim 300\text{Ks}^{-1}$ ) from austenitizing temperature ( $1000^\circ\text{C}$ , 10 minutes), the specimens were 13mm in length and 1.1mm in diameter. Lattice parameter measurements were carried out using a X-ray diffractometer with Fe-filtered  $\text{CoK}_\alpha$  radiation. The precision ferrite lattice parameter determination included a knowledge of the angular positions of the (110), (200), (211) and (220) peaks. The data were analysed using a Taylor-Sinclair function to extrapolate the values of the ferrite parameter to angular position of  $\Theta=90^\circ$ . The linear expansion coefficient of ferrite ( $e_\alpha$ ) was determined by annealing a specimen at  $650^\circ\text{C}$  for 30 minutes to decompose any retained austenite and then recording the change of length during slow cooling. The linear expansion coefficient of austenite ( $e_\gamma$ ) was measured after cooling from temperature of  $1100^\circ\text{C}$  while the specimen was in the single  $\gamma$  phase field. Determination of the linear expansion coefficients was carried out in a UBD Leitz-Wetzlar dilatometer. Thin foils were stored in ethanol and subsequently examined in a Tesla BS-540 electron microscope at an operating voltage of 120 kV.

## 3. Conversion of dilatometry data

For the transformation of austenite into a mixture of bainitic ferrite and carbon enriched residual austenite and assuming isotropic strain the relationship between dimensional changes  $\Delta L$  and volume changes  $\Delta V$  is given by the equation [4]:

$$\frac{\Delta V}{V} \approx 3 \frac{\Delta L}{L} \quad (1)$$

Where  $L$  is the specimen length at the transformation temperature. The lattice parameters of bainitic ferrite and untransformed austenite at the reaction temperature,  $a_\alpha$  and  $a_\gamma$ , can be calculated from the values of lattice parameters at ambient temperature ( $25^\circ\text{C}$ , 298K) using the linear thermal expansion coefficients  $e_\alpha$  and  $e_\gamma$ :

$$a_\alpha = a_{0\alpha} [1 + e_\alpha ( T - 298 )] \quad (2)$$

$$a_\gamma = a_{0\gamma} [1 + e_\gamma ( T - 298 )] \quad (3)$$

where  $T$  is the absolute temperature. The room temperature lattice parameter of austenite ( $a_{0\gamma}$  in nm) at the mean steel composition (i.e. when  $V_\alpha = 0$ ) can be calculated using equation determined by Dyson and Holmes [8]:

$$a_{o\gamma} = 0.3578 + \sum_{i=1}^n C_i x_i \quad (5)$$

where  $C_i$  are coefficients and  $x_i$  is the weight fraction of alloying element in phase  $\gamma$ , where  $i = 1, 2, \dots, n$  represents alloying elements ( $i = 1$  for carbon,  $i > 1$  for substitutional solutes). The ferrite lattice parameter  $a_{o\alpha}$  was determined by X-ray analysis and for ascertain it was calculated using following equation [4]:

$$a_{o\alpha} = 0.28664 + (3a_{Fe}^2)^{-1} \cdot [(a_{Fe} - 0.0279x_c^\alpha)^2 (a_{Fe} + 0.2496x_c^\alpha) - a_{Fe}^3] - 0.003x_{Si}^\alpha + 0.006x_{Mn}^\alpha + 0.007x_{Ni}^\alpha + 0.031x_{Mo}^\alpha + 0.005x_{Cr}^\alpha + 0.0096x_V^\alpha \quad (6)$$

The lattice parameter of pure ferrite was taken as  $a_{Fe} = 0.28664 \text{ nm}$  [16]. The terms  $x_i^\alpha$  represent the mole fraction of the species  $i$  in phase  $\alpha$ . The carbon concentration of the residual austenite  $x_1^\gamma$  increases during bainitic transformation as a consequence of the increasing volume fraction of bainitic ferrite. Given that the excess carbon in the bainite ferrite partitions into the residual austenite and assuming that the final microstructure consists of only bainitic ferrite and residual austenite it is possible to estimate the carbon concentration according to the following relationship derived from mass balance considerations [4]:

$$x_1^\gamma = \frac{2a_\alpha^3 \bar{x} (1 - x_1^\alpha)(1 - V_\alpha) + a_{e\gamma}^3 (\bar{x} - x_1^\alpha) V_\alpha}{2a_\alpha^3 (1 - x_1^\alpha)(1 - V_\alpha) + a_{e\gamma}^3 (\bar{x} - x_1^\alpha) V_\alpha} \quad (7)$$

The carbon content of the ferrite  $x_1^\alpha$ , is a very small and is approximated by the  $A_1 \alpha/(\alpha+\gamma)$  phase boundary of the Fe-C phase diagram (since of its smallness ignoring the effect of substitutional elements). The value of carbon in bainitic ferrite was taken to be  $x_1^\alpha = 0.00139$  (0.03 wt.%) [16]. The calculated carbon concentrations of residual austenite at the point where the formation of bainite terminates will be next compared against the extrapolated  $T_0$ ,  $T_0'$  and  $A_3'$  phase boundaries.

#### 4. Material, results and discussion

The composition of the steel investigated is given in Tab. 1.

Tab. 1. Chemical compositions of the steel used in this study.  
All concentrations are given in wt.% and at.% ( $\times 10^{-2}$ )

| Steel |      | C     | Si    | Cr    | Mn    | Mo    | Al    |
|-------|------|-------|-------|-------|-------|-------|-------|
| 15HM2 | wt.% | 0.14  | 0.23  | 0.88  | 0.73  | 2.4   | 0.03  |
|       | at.% | 0.651 | 0.457 | 0.945 | 0.729 | 1.397 | 0.062 |

The dilatometry results showed that the relative length change during the formation of bainite at selected temperatures increases as the isothermal transformation temperature decreases below the  $B_S$  (Fig. 1), then the amount of bainite formed is dependent on the transformation temperature. The lattice parameters of ferrite and austenite and values of linear expansion coefficients are given in Tab. 2. The

details for calculation of volume fraction of transformation are given in Tab. 3.

Calculated and measured the carbon concentration of the residual austenite ( $x_\gamma$ ) and carbon concentration at the interphase boundaries in Fe-Cr-Mo-C steel are given in Tab. 4.

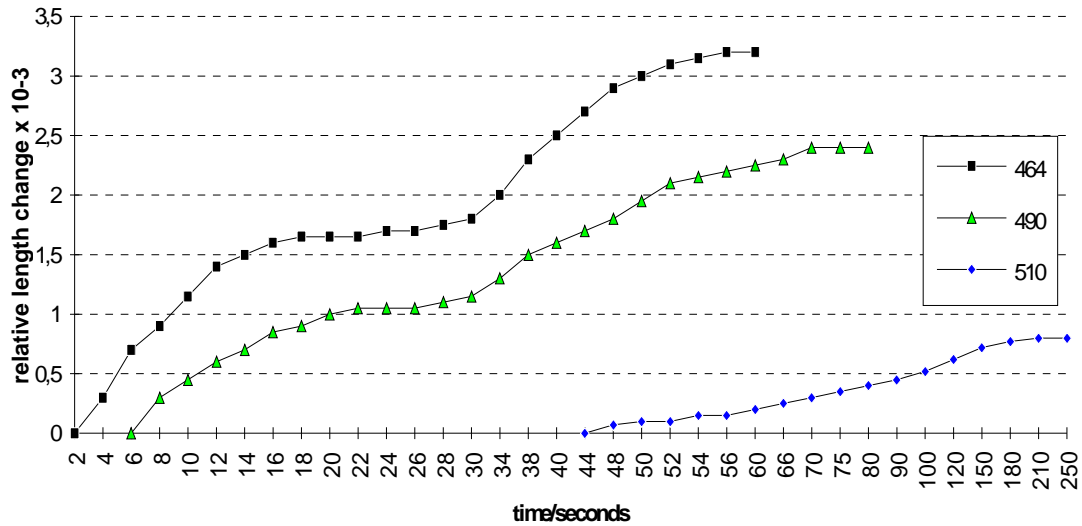


Fig. 1. The relative length change ( $\Delta L/L$ ) observed by dilatometry during isothermal transformation at selected temperatures below  $B_S$  temperature in Fe-Cr-Mo-C steel

Tab. 2. Lattice parameters and linear expansion coefficients of ferrite and austenite

| Steel      | Lattice parameter of ferrite $a_{\alpha}$<br>nm | Lattice parameter of austenite $a_{\gamma}$<br>nm | Ferrite $e_\alpha$<br>$^{\circ}\text{C}^{-1}$ ,<br>$\times 10^{-5}$ | Austenite $e_\gamma$<br>$^{\circ}\text{C}^{-1}$ ,<br>$\times 10^{-5}$ |
|------------|---|---|---|---|
| Fe-Cr-Mo-C | 0.2872<br>0.2871 *                              | 0.35910   | 1.627   | 2.317   |

\* The ferrite lattice parameter determined using a X-ray diffractometer

Tab. 3. Parameters for determination of volume fractions of bainite ( $V_B$ ) in Fe-Cr-Mo-C steel

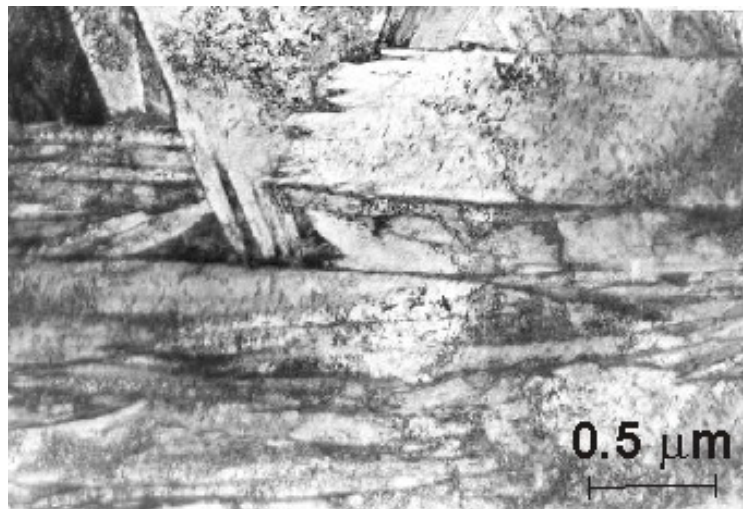
| Transformation temperature, $^{\circ}\text{C}$ | $a_\gamma$<br>nm | $a_\alpha$<br>nm | $\Delta L/L^*$<br>$\times 10^{-3}$ | $V_B$ |
|--|------------------|------------------|------------------------------------|-------|
| 464  | 0.3627           | 0.2893           | 4.88                               | 0.66  |
| 475  | 0.3628           | 0.2893           | 4.52                               | 0.62  |
| 490  | 0.3629           | 0.2894           | 4.56                               | 0.53  |
| 500  | 0.3630           | 0.2894           | 4.35                               | 0.22  |
| 510  | 0.3631           | 0.2895           | 4.46                               | 0.18  |

\* Values of the dimensional changes accompanying the transformation of austenite to bainitic ferrite measured at transformation temperature,

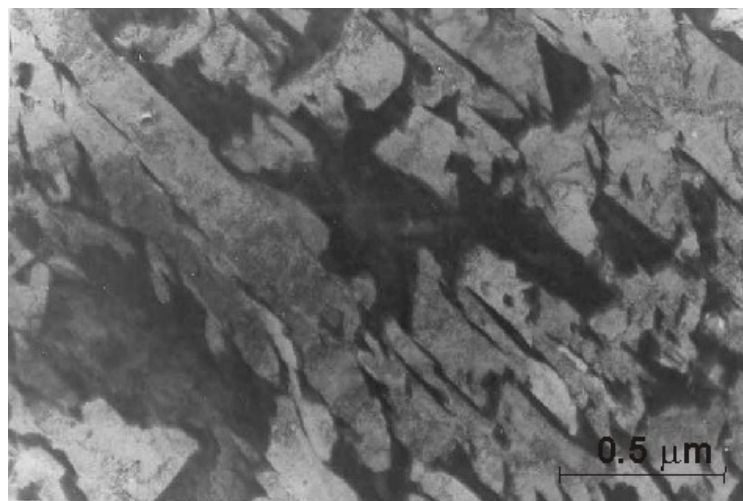
$V_B$  Measured volume fraction of transformation.

Fig. 2 shows the general morphology of the microstructure in 15HM2 steel after austenitization at 1200°C and isothermal transformation at 450°C for 600s. The morphology of the bainite is similar to low carbon lath martensite, where dislocated laths are separated by films of retained austenite. No blocky austenite was observed in this structure. Careful examination of this microstructure shows small precipitated carbides laying inside bainitic ferrite laths. No significant changes in morphology with increasing reaction time were observed after isothermal transformation at 450°C. This structure, therefore, belongs to lower bainite assuming that lower bainite in this steel is a structure composed of carbides within bainitic laths with interlath retained austenite films [11-15].

After austenitization at 1200°C and at higher transformation temperature (550°C), bainite changes into a morphology without carbides within the laths but with blocky retained austenite (Fig. 3).



*Fig. 2. Morphology of the microstructure in 15HM2 steel after austenitization at 1200°C and isothermal transformation at 450°C for 600s. Thin foil*



*Fig. 3. Microstructure of 15HM2 steel after austenitization at 1200°C and isothermal transformation at 550°C for 1800s. Thin foil*

Tab. 4. Calculated and measured the carbon concentration of the residual austenite ( $x_\gamma$ ) and carbon concentration at the interphase boundaries in Fe-Cr-Mo-C steel

| Phase      | Transformation temperature, °C / Carbon concentration at the interphase, mol |        |        |        |        |        |        |        |
|------------|--|--------|--------|--------|--------|--------|--------|--------|
|            | 700  | 600    | 510    | 500    | 490    | 475    | 464    | 400    |
| $A_3'$     | 0.0233   | 0.0520 | 0.0840 | 0.0878 | 0.0918 | 0.0978 | 0.1023 | 0.1257 |
| $x_{T_0}$  | 0.008  | 0.0157 | 0.0243 | 0.0253 | 0.0261 | 0.0277 | 0.0293 | 0.0384 |
| $x_{T_0'}$ |  | 0.0033 | 0.0135 | 0.0147 | 0.0160 | 0.0179 | 0.0194 | 0.0267 |
| $x_\gamma$ |  |        | 0.0076 | 0.0079 | 0.0121 | 0.0146 | 0.0162 |        |

The determined carbon concentrations of the residual austenite at the point where the formation of bainite ceases are compared with the  $T_0$ ,  $T_0'$  and  $A_3'$  phase boundaries for examined 15HM2 steel in Fig. 4. The diagram was calculated using a model developed by Bhadeshia [4,5] based on the McLellan and Dunn quasi-chemical thermodynamic model [16]. The  $T_0$  curve represents the locus of all points where austenite and ferrite of the same composition have equal free energy [1,4]. The  $T_0'$  curve allows for 400J/mol of stored energy in the bainitic ferrite to take account of the strain energy due to the invariant-plane strain shape change that accompanies the growth of bainitic ferrite [5,7]. The  $A_3'$  curve is the calculated paraequilibrium ( $\alpha+\gamma$ )/ $\gamma$  phase boundary indicating equilibrium between ferrite and austenite when the ratio of substitutional alloying elements to iron is constant everywhere. The bainite and martensite reactions start temperatures  $B_S$  and  $M_S$  are also marked on that diagram.

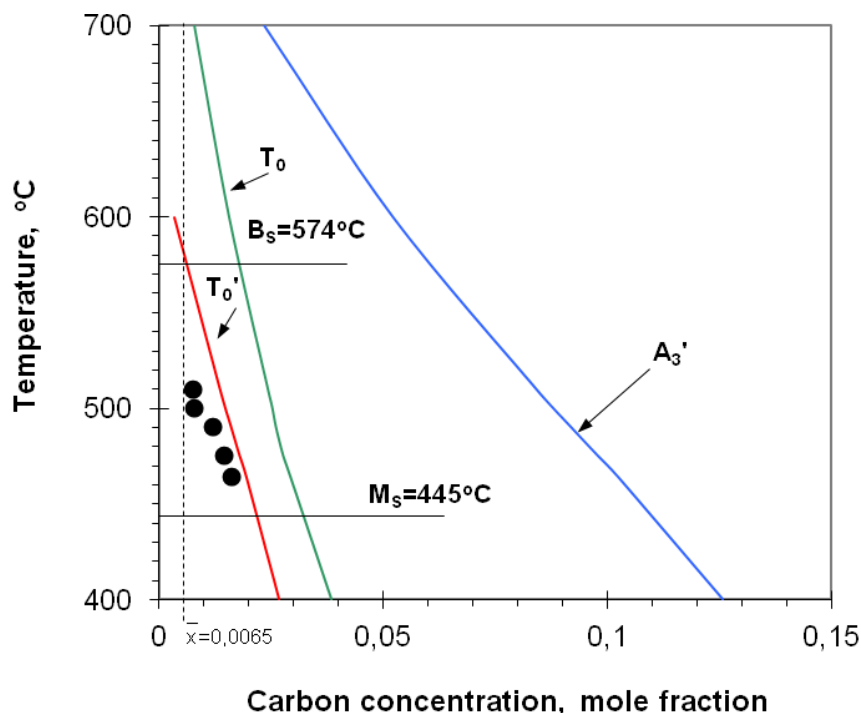


Fig. 4. Calculated phase diagram with experimental data of carbon concentration of residual austenite at the termination of isothermal bainite formation for Fe-Cr-Mo-C steel (black circles represent experimental data)

Paraequilibrium is a constrained equilibrium in which only carbon atoms are free to partition between ferrite and austenite. The ratio of the substitutional solute concentration to the iron concentration is the same in ferrite and in austenite, the chemical potential of carbon is equal in the two phases [6]. The paraequilibrium phase boundary is chosen because no substitutional alloying element partitioning occurs during bainite formation.

If the hypothesis that paraequilibrium exists during all stages of transformation is correct, then the reaction should stop when the carbon concentration of the austenite is given by the  $A_3'$  curve. In presented experiment the reaction is found to stop when the average carbon concentration of the residual austenite is close to the  $T_0$  curve than the  $A_3'$  boundary (black circles in Fig. 4). Note that the difference in carbon concentrations between the  $T_0'$  and  $A_3'$  curves at the chosen temperatures of bainitic reaction is very large, so the presented experiment is a sensitive indication of the failure of the transformation to reach paraequilibrium. The  $T_0'$  curve has a negative slope, so the austenite can tolerate more carbon before diffusionless transformation becomes impossible, as the transformation temperature is reduced.

The presented above results can be explained when it is assumed that bainitic ferrite grows without diffusion, but any excess of carbon is soon afterwards rejected into the residual austenite by diffusion [9-13]. This makes more difficult for subsequent bainitic ferrite to grow, when the austenite becomes stabilised by increased carbon concentration. The maximum extent to which the bainite reaction can proceed is therefore determined by the composition of the residual austenite. A stage where diffusionless growth becomes thermodynamically impossible and the formation of bainitic ferrite terminates is where the carbon concentration of the austenite reaches the  $T_0'$  curve. The incomplete reaction phenomenon supports the hypothesis that the growth of bainitic ferrite occurs without any diffusion with carbon being partitioned subsequently into the residual austenite. There is as yet no reasonable alternative explanation of this phenomenon.

## 5. Conclusions

The austenite to bainite transformation was studied in Fe-Cr-Mo-C steel using dilatometry backed by thermodynamic analysis. The results obtained are summarized as follows:

1. The reaction terminates prematurely as the carbon content of the residual austenite reaches the  $T_0'$  curve well before the paraequilibrium carbon concentration is achieved (given by the extrapolated  $A_3'$  phase boundary) which indicates that the growth of bainitic ferrite is diffusionless.
2. The maximum extent of bainite formation in 15HM2 steel is dependent on the transformation temperature and the degree of transformation strongly decreases with approaching the bainite start temperature.

## References

- [1] Aaronson, H.I., Reynolds, W.T., Shiflet, G.J., Spanos, G., *Bainite Viewed Three Different Ways*, Metall. Trans. A, 21A, 1343-1380, 1990.
- [2] Aaronson, H.I., *The proeutectoid ferrite and the proeutectoid cementite reactions*, In: Aaronson HI, Zackay VF, editors. *Decomposition of Austenite by Diffusional Processes*. New York: Interscience Publishers, 387-546, 1962.
- [3] Aaronson, H.I., *The Mechanism of Phase Transformations in Crystalline Solids*, The Institute of Metals, London, 1969, p.270.
- [4] Bhadeshia, HKDH, Christian, JW., *Bainite in steels*, Metall Trans. A, 21A, 767-797, 1990.

- [5] Caballero, F.G., Miller, M.K., Babu, S.S., Garcia-Mateo, C., *Atomic scale observations of bainite transformation in a high carbon high silicon steel*, Acta Materialia, 55, 381-390, 2007.
- [6] Chen, J.K., Vandermeer, R.A., Reynolds, W.T., JR., *Effect of Alloying Elements upon Austenite Decomposition in Low-C Steels*, Metall. Mater. Trans.A, 25A, 1367-1379, 1994.
- [7] Christian J.W., Edmonds D.V., *Int. Conf. on Phase Transformations in Ferrous Alloys*, A.R. Marder, J.I. Goldstein, ASM, Metals Park, OH, 1984, p.293.
- [8] Dyson D.J., Holmes, B., *Effect of alloying additions on the lattice parameter of austenite*, J. Iron Steel Inst., 208, 469-474, 1970.
- [9] Hehemann, R.F., Kinsman, K.R., Aaronson, H.I., *A debate on the bainite reaction*, Metall. Trans., 3, 1077-94, 1972.
- [10] Hillert, M., Höglund, L., Ägren, J., *Escape of carbon from ferrite plates in austenite*, Acta Metall Mater., 41, 1951-7, 1993.
- [11] Ławrynowicz, Z., Barbacki, A., *Carbides precipitation in bainite in an experimental Mo-Cr-V-Ti steel*, Conference Proceedings of the 6-th International Conference "Carbides, Nitrides, Borides," Poznań-Kołoobrzeg, pp. 42-47, 1993.
- [12] Ławrynowicz, Z., *Ausferritic or Bainitic Transformation in ADI*, Proceedings of the 12th International Symposium on Advanced Materials, Paper No: 98, ISAM2011-98, Rawalpindi, Pakistan.
- [13] Ławrynowicz, Z., *Decarburisation of bainitic ferrite laths and its influence on the microstructure in Fe-Cr-Si-C steel*, Advances in Materials Science, 2011, Vol. 11, No. 2 (28), June pp. 56-64, 2011.
- [14] Ławrynowicz, Z., *Affect of decarburisation times of bainitic ferrite laths on the microstructure in Fe-Cr-C steel*, Journal of Polish CIMAC, Vol. 6, No. 3, pp. 127-136, 2011.
- [15] Ławrynowicz, Z., *Affect of cementite precipitation on the extend of bainite transformation in Fe-Cr-C steel*, Advances in Materials Science, Vol. 11, No. 3 (29), pp.13-19, September 2011.
- [16] McLellan, R.B., Dunn, W.W., J.Phys.Chem. Solids, 30, 2631-2637, 1969.
- [17] Reynolds, W.T. et al., *An investigation of the Generality of Incomplete Transformation to Bainite in Fe-C-X Alloys*, Metall. Trans.A, 21A, 1479-1491, 1990.